IAES International Journal of Robotics and Automation (IJRA)
Vol. 12, No. 3, September 2023, pp. 228~239
ISSN: 2722-2586, DOI: 10.11591/ijra.v12i3.pp228-239

Fault tolerance of a quadrotor via feedback linearization approach

Ali Jebelli[1], Alireza Najafiyanfar[2], Arezoo Mahabadi[3], Mustapha C. E. Yagoub[4]
[1]Department of Mechanical Engineering, University of Alberta, Ottawa, Canada
[2]Faculty of Electrical Engineering, K.N. Toosi University of Technology, Tehran, Iran
[3]Department of Basic Engineering Science, Tehran University, Tehran, Iran
[4]School of Electrical Engineering and Computer Science, University of Ottawa, Canada

Article Info

Article history:

Received Jan 23, 2023
Revised Apr 8, 2023
Accepted Apr 24, 2023

Keywords:

Disturbance
Fault tolerance
Feedback linearization
Quadcopters
State space
Unmanned aerial vehicle

ABSTRACT

A control algorithm is proposed to efficiently control the state, position, and height of a nonlinear dynamic model of a quadcopter. Based on feedback linearization, a state space model is presented for the system with the controller with a two-loop control structure designed and implemented in it. The inner and faster controller is responsible for adjusting the quadcopter height and angles, and the outer and slower controller is responsible for changing the desired figures of roll and pitch angles to control the system position. Whenever a rotor of the quadcopter rotor fails, the status and position of the system are converged and the system is stabilized. Simulation results based on different scenarios indicate the proper performance of the control system whenever there are external disturbances. Note that the gyroscopic effects because of the propeller rotation were not considered.

Corresponding Author:

Ali Jebelli
Department of Mechanical Engineering, University of Alberta
Edmonton, AB, Canada
Email: jebelli@ualberta.ca

1. INTRODUCTION

Present day, extensive work has been done in the field of unmanned aerial vehicles, leading to a significant increase in both academic research and industrial projects. Various control methods including sliding model [1], [2], backtracking [3], adaptive [4], adaptive backtracking [5], resistant proportional integral derivative (PID) [6], and linear quadratic Gaussian (LQG) [7] have been utilized in quadcopter systems to control the status and position of the quadcopter. On the other side, the issues of fault detection and fault-tolerant control of the faults within sensors, rotors, or other parts of the quadcopter have been discussed. There are two types of fault-tolerant control systems: passive and active [8]. The control structure of a passive control system does not change, i.e., the control system is resistant to faults whenever there is a fault while the control system of an active control system is reset whenever there is a fault [9]. Several methods have been presented to design the controllers in case of rotor failure in the fault-tolerant control system. Sliding mode control has been used to control the operating conditions in the case of disturbance and rotor failure [10], [11]. Model predictive control has been used to control the system [12]–[14]. Robust adaptive control has been used to track the height and status of the quadcopter; moreover, the tracking fault is converged in the case of rotor failure [15]. A nonlinear adaptive discrete algorithm and a PID algorithm have been used in inner and outer loops, respectively, to control route tracking [16]. Optimization methods have been used to minimize the force being applied by the rotors in the case of their failure [17]. Intelligent control methods such as reinforcement learning [18] have also been used for fault-tolerant. An intelligent logic algorithm has been used to control a hexadrone; moreover, it has been shown that the control algorithm has a proper performance in the case of two rotors' failure [19].

In this research, a nonlinear model for the quadcopter is first introduced, and then, in order to design the controller, a state space model for the system is presented using the feedback linearization method, in which the gyroscopic effects because of the rotation of the propeller have been ignored. The fault-tolerant controller has a two-loop control structure in which the inner and faster controller is responsible for adjusting the quadcopter height and angles while the outer and slower controller is responsible for changing the desired figures of roll and pitch angles to control the system position. The controllers have been applied to the nonlinear system to investigate performance within different scenarios. In this article, after the mathematical modeling of a quadrotor, the state space model of the system is presented, then the details of the design of the internal and external controller are presented, and the simulation results and comparison of different states are presented.

2. MATHEMATICAL MODEL

A quadrotor is an unmanned aerial vehicle (UAV) with six degrees of freedom. It accounts for two pairs of rotors that rotate in opposite directions. The dynamical model of the given quadcopter is presented in Figure 1, where the state vector $[x, y, z]$ indicates the position of the center of the gravity of the quadcopter and its linear velocity in the body-frame is indicated by the vector $[\dot{x}, \dot{y}, \dot{z}]$; the Euler angles $[\varphi, \theta, \psi]$ indicates the roll, the pitch, and the yaw, respectively, and $[p, q, r]$ represents its angle velocity in the body-frame. The dynamic equations are expressed in function of the ground frame and the body frame as (1) to (6) [20].

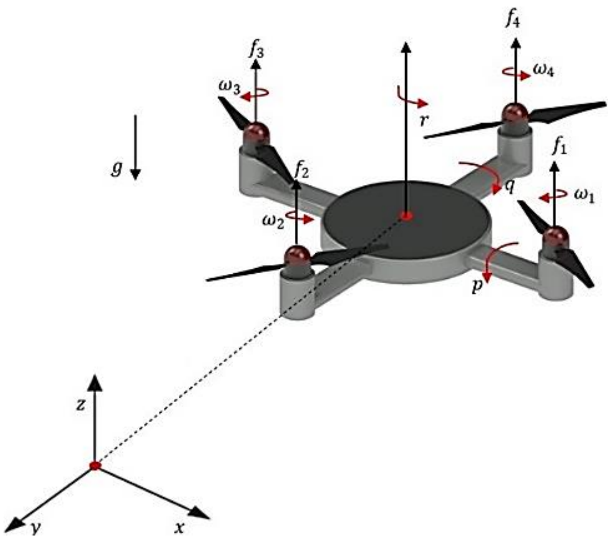

Figure 1. Quadcopter UAV

$$\ddot{x} = \frac{cos(\varphi)\, cos(\psi)\, sin(\theta) + sin(\varphi)\, sin(\psi)}{m} u_1 - \frac{a_2}{m}\dot{x} + d_x \tag{1}$$

$$\ddot{y} = \frac{cos(\varphi)\, sin(\psi)\, sin(\theta) - cos(\psi)\, sin(\varphi)}{m} u_1 - \frac{a_2}{m}\dot{y} + d_y \tag{2}$$

$$\ddot{z} = \frac{1}{m}(u_1\, cos(\varphi)\, cos(\theta) - a_2\dot{z} - mg) + d_z \tag{3}$$

$$\dot{p} = \frac{1}{I_{xx}}\left(-a_1 p - qr(I_{zz} - I_{xx}) + u_2 - I_{zz}\dot{\theta}\omega_r\right) + d_\varphi \tag{4}$$

$$\dot{q} = \frac{1}{I_{xx}}\left(-a_1 q - pr(I_{xx} - I_{zz}) + u_3 + I_{zz}\dot{\phi}\omega_r\right) + d_\theta \tag{5}$$

$$\dot{r} = \frac{1}{I_{zz}}(-a_1 r + u_4) + d_\psi \tag{6}$$

In (1) to (6), m represents the quadcopter mass, g is the accelerant of gravity, and l is the distance from each rotor to the center of gravity. The vector $d = [d_x, d_y, d_z, d_\emptyset, d_\theta, d_\psi]$ represents the wind disturbance and $\omega_r = (\omega_1 + \omega_2 + \omega_3 + \omega_4)$ represents the overall residual rotor angular velocity, where $\omega_1, \omega_2, \omega_3$, and ω_4 stand for the angular speed of the propellers. Also, the control inputs u_1, u_2, u_3, and u_4 can be obtained from the matrix equation in (7).

$$\begin{bmatrix} u_1 \\ u_2 \\ u_3 \\ u_4 \end{bmatrix} = \begin{bmatrix} 1 & 1 & 1 & 1 \\ -l & 0 & l & 0 \\ 0 & l & 0 & -l \\ 1 & -1 & 1 & -1 \end{bmatrix} \begin{bmatrix} \omega_1^2 \\ \omega_2^2 \\ \omega_3^2 \\ \omega_1^2 \end{bmatrix} \tag{7}$$

It is supposed that the dynamic model of the quadrotor structure provided in (1) to (6) is rigid and symmetric, the body frame's origin is the same as the gravity's center, and the body frame's axes coincide with the quadrotor inertia axes.

2.1. State space model

Let $\boldsymbol{x} = [\varphi, \theta, \psi, p, q, r, x, y, z, \dot{x}, \dot{y}, \dot{z}]$ be the state vector and $u = [u_1, u_2, u_3, u_4]$ the input vector. Considering that in the case where all the rotors are working, ω_r is zero, and in the case of an engine failure, the values of $I_{zz}\dot{\theta}\omega_r$ and $I_{zz}\dot{\emptyset}\omega_r$ are very small, we ignore the gyroscopic effects because of the propeller rotation [21, 22], and the dynamic equations in (1) to (6) can be adjusted in a state space model as (8) to (19).

$$\dot{x}_1 = x_4 + x_5 \sin(x_1)\tan(x_2) + x_6 \cos(x_1)\tan(x_2) \tag{8}$$

$$\dot{x}_2 = x_5 \cos(x_1) - x_6 \sin(x_1) \tag{9}$$

$$\dot{x}_3 = \frac{1}{\cos(x_2)}(x_5 \cos(x_1) + x_6 \sin(x_1)) \tag{10}$$

$$\dot{x}_4 = \frac{1}{I_{xx}}(-a_1 x_4 - x_5 x_6 (I_{zz} - I_{xx}) + u_2) + d_\varphi \tag{11}$$

$$\dot{x}_5 = \frac{1}{I_{xx}}(-a_1 x_5 - x_4 x_6 (I_{xx} - I_{zz}) + u_3) + d_\theta \tag{12}$$

$$\dot{x}_6 = \frac{1}{I_{zz}}(-a_1 x_6 + u_4) + d_\psi \tag{13}$$

$$\dot{x}_7 = x_{10} \tag{14}$$

$$\dot{x}_8 = x_{11} \tag{15}$$

$$\dot{x}_9 = x_{12} \tag{16}$$

$$\dot{x}_{10} = \frac{\cos(x_1)\cos(x_2)\sin(x_3) + \sin(x_1)\sin(x_3)}{m} u_1 - \frac{a_2}{m} x_{10} + d_x \tag{17}$$

$$\dot{x}_{11} = \frac{\cos(x_1)\sin(x_2)\sin(x_3) - \cos(x_3)\sin(x_1)}{m} u_1 - \frac{a_2}{m} x_{11} + d_y \tag{18}$$

$$\dot{x}_{12} = \frac{1}{m}(u_1 \cos(x_1)\cos(x_2) - a_2 x_{12} - mg) + d_z \tag{19}$$

2.2. Inner control loop

Let $\bar{x}$ represents the dynamics of the state variables $(x_1, x_2, x_3, x_4, x_5, x_6\ x_9, x_{12})$. The state space model can be formulated as (20),

$$\dot{x} = f(\bar{x}) + g(\bar{x})u \tag{20}$$

and the state variables x_1, x_2, x_3, x_9 could be written as (21),

$$\begin{bmatrix}\dot{x}_1\\ \dot{x}_2\\ \dot{x}_3\\ \dot{x}_9\end{bmatrix} = \begin{bmatrix} x_4 + x_5\sin(x_1)\tan(x_2) + x_6\cos(x_1)\tan(x_2)\\ x_5\cos(x_1) - x_6\sin(x_1)\\ \dfrac{1}{\cos(x_2)}(x_5\cos(x_1) + x_6\sin(x_1))\\ x_{12}\end{bmatrix} = \hat{f}(\bar{x}) \tag{21}$$

which is independent of the input of the system. This property will become useful while the second derivative of $[x_1, x_2, x_3, x_9]^T$ is being calculated as (22),

$$\begin{bmatrix}\ddot{x}_1\\ \ddot{x}_2\\ \ddot{x}_3\\ \ddot{x}_9\end{bmatrix} = \frac{d\hat{f}(\bar{x})}{dt} = \frac{\partial\hat{f}(\bar{x})}{\partial\bar{x}}\dot{\bar{x}} = J(\bar{x})f(\bar{x}) + J(\bar{x})g(\bar{x})u \tag{22}$$

where $J(\bar{x})$ denotes the Jacobian matrix $\frac{\partial\hat{f}(\bar{x})}{\partial\bar{x}}$. If and only if $x_2 \neq \arctan\left(\frac{I_{zz}l}{2I_{xx}d}\right)\cos(x_1)$, it can be proved that the matrix $J(\bar{x})g(\bar{x})$ is invertible. This condition is satisfied in most practical scenarios. Consider $x_{id}, \dot{x}_{id}, \ddot{x}_{id}$ the desired values for $x_i, \dot{x}_i, \ddot{x}_i$ and let us define the i$^{\text{th}}$ error as $e_i = x_i - x_{id}$. If the control inputs are selected as (23),

$$u^* = -(J(\bar{x})h(\bar{x}))^{-1}(J(\bar{x})h) + (J(\bar{x})h(\bar{x}))^{-1}\left(\begin{bmatrix}\ddot{x}_{1d}\\ \ddot{x}_{2d}\\ \ddot{x}_{3d}\\ \ddot{x}_{9d}\end{bmatrix} - \begin{bmatrix}ki_1^1e_1\\ ki_2^1e_2\\ ki_3^1e_3\\ ki_9^1e_9\end{bmatrix} - \begin{bmatrix}ki_1^2\dot{e}_1\\ ki_2^2\dot{e}_2\\ ki_3^2\dot{e}_3\\ ki_9^2\dot{e}_9\end{bmatrix}\right) \tag{23}$$

with ki_i^j is the positive parameters, then the error dynamic is expressed as (23),

$$\begin{bmatrix}\ddot{e}_1\\ \ddot{e}_2\\ \ddot{e}_3\\ \ddot{e}_9\end{bmatrix} + \begin{bmatrix}ki_1^1e_1\\ ki_2^1e_2\\ ki_3^1e_3\\ ki_9^1e_9\end{bmatrix} + \begin{bmatrix}ki_1^2\dot{e}_1\\ ki_2^2\dot{e}_2\\ ki_3^2\dot{e}_3\\ ki_9^2\dot{e}_9\end{bmatrix} = \begin{bmatrix}0\\0\\0\\0\end{bmatrix} \tag{24}$$

which yields the exponential stability of second-order dynamics.

2.3. Outer control loop

Since the roll and pitch angles determine the direction, an outer control loop will be computed whose job it is to calculate the desired values for the roll and pitch angles to track a desired position in the horizontal plane. The subsystems whose dynamics are represented by the state variables $x_1, x_2, x_3, x_4, x_5, x_6\ x_9, x_{12}$ are represented by the constants ki and ko. To avoid losing the system's stability, it is required to choose $ko \ll ki$ that causes the inner control loop to act much faster than the outer control loop. By presuming that x_1 and x_2 are small angles, x_{1d} and x_{2d} are selected close to zero as (22),

$$\begin{bmatrix}x_{1d}\\ x_{2d}\end{bmatrix} = -\frac{m}{u_1}\begin{bmatrix}\sin(x_3) & -\cos(x_3)\\ \cos(x_3) & \sin(x_3)\end{bmatrix}\begin{bmatrix}-\dfrac{a_2}{m}x_{10} + ko_1^1e_{10} + ko_1^2e_7 - \dot{x}_{10d}\\ -\dfrac{a_2}{m}x_{10} + ko_2^1e_{10} + ko_2^2e_7 - \dot{x}_{10d}\end{bmatrix} \tag{25}$$

where ko_i^j is positive constants. Then, the error dynamic for the horizontal displacements in a closed loop is (26).

$$\begin{bmatrix}-\dfrac{a_2}{m}x_{10} + ko_1^1e_{10} + ko_1^2e_7 - \dot{x}_{10d}\\ -\dfrac{a_2}{m}x_{10} + ko_2^1e_{10} + ko_2^2e_7 - \dot{x}_{10d}\end{bmatrix} = \begin{bmatrix}0\\0\end{bmatrix} \tag{26}$$

Practically, when occurring fault for rotors, the roll, pitch, yaw, and altitude are stabilized by the inner control law, while the near hover condition is exploited by the pouter control law to slowly change the pitch and roll angles in order to reach the system to the desired position.

3. RESULTS AND DISCUSSION

This section evaluates the performance of the proposed controller in the presence of disturbances by simulation with initial states x_0=[0, 0, 0, 0, 0, 0, 0, 0, 2, 0, 0, 0] in MATLAB software. Three cases were considered to evaluate the controllers. In the first case, the quadrotor does the task without motor failure and disturbance. In the second case, one rotor of the quadrotor is turned off from the beginning. In the third case, in addition to one rotor of the quadrotor being turned off from the beginning, there are external disturbances. The physical parameters of the quadrotor are set as (27).

$$\begin{aligned} &m = .5\,kg, l = .25\,m, g = 9.81\,ms^{-2} \\ &a_1 = a_2 = 1e-2 \\ &Ixx = 5e-3\,kgm^2 \\ &Iyy = 5e-3\,kgm^2 \\ &Izz = 1e-2\,kgm^2 \end{aligned} \tag{27}$$

3.1. Test 1 (test without rotor failure and disturbance)

In this test, it has been assumed that none of the system rotors failed and there is no disturbance in the system. As shown in Figures 2 and 3, the system has reached the desired values, that is to say, has been stabilized. The angular velocity of the rotors is indicated in Figure 4, as clear rotors work without failure.

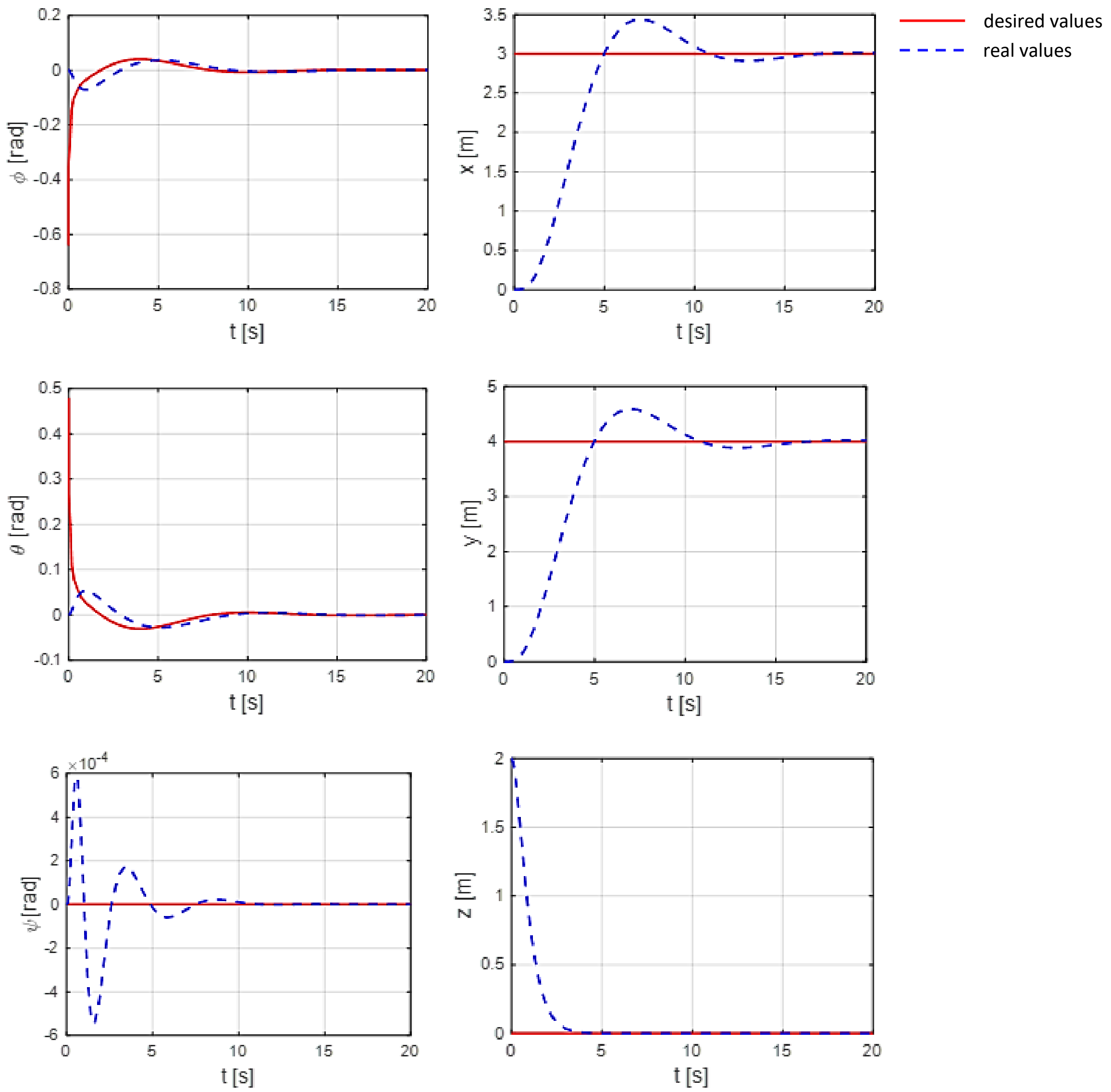

Figure 2. Position and Euler angles

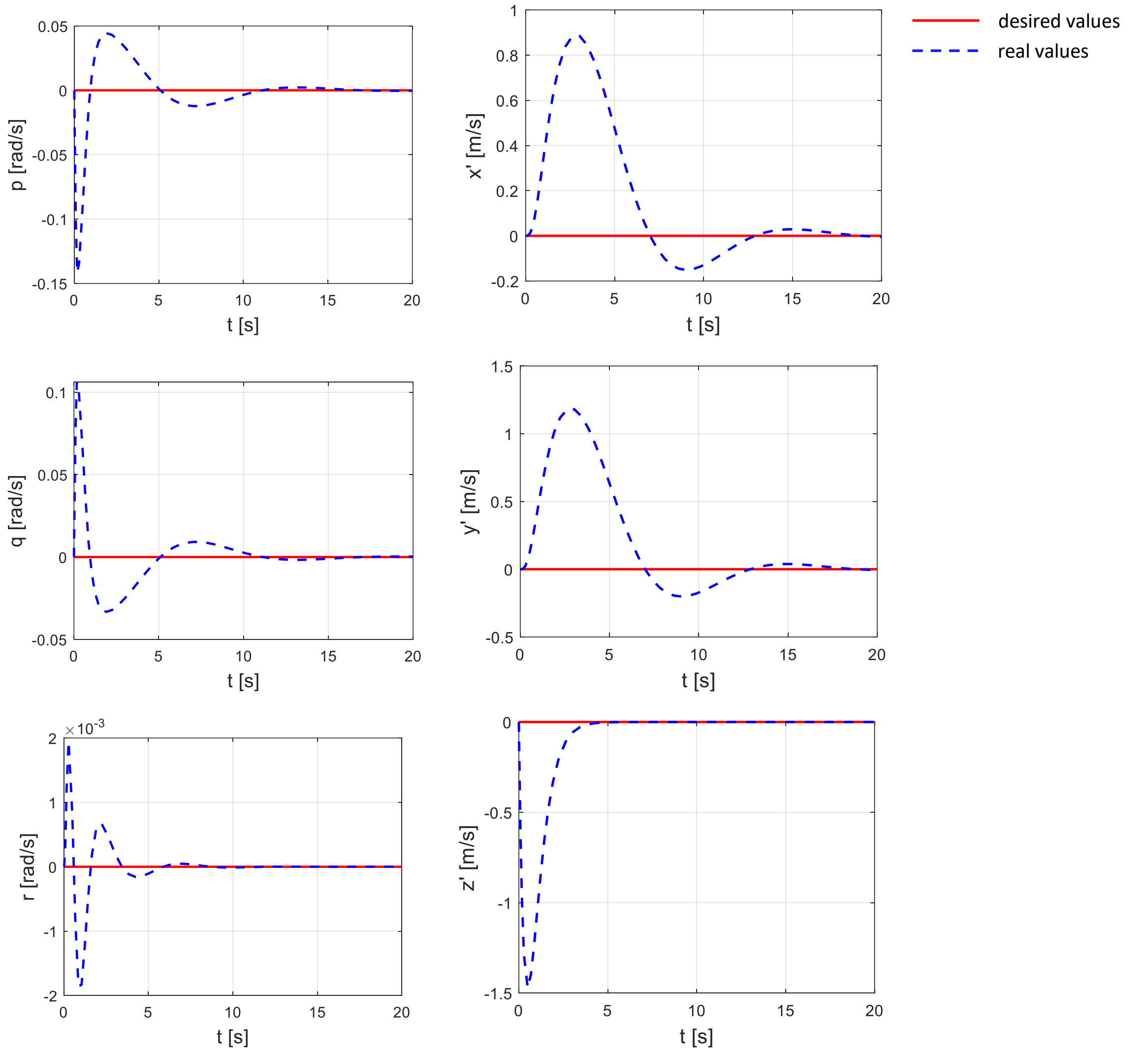

Figure 3. Linear and angular velocity

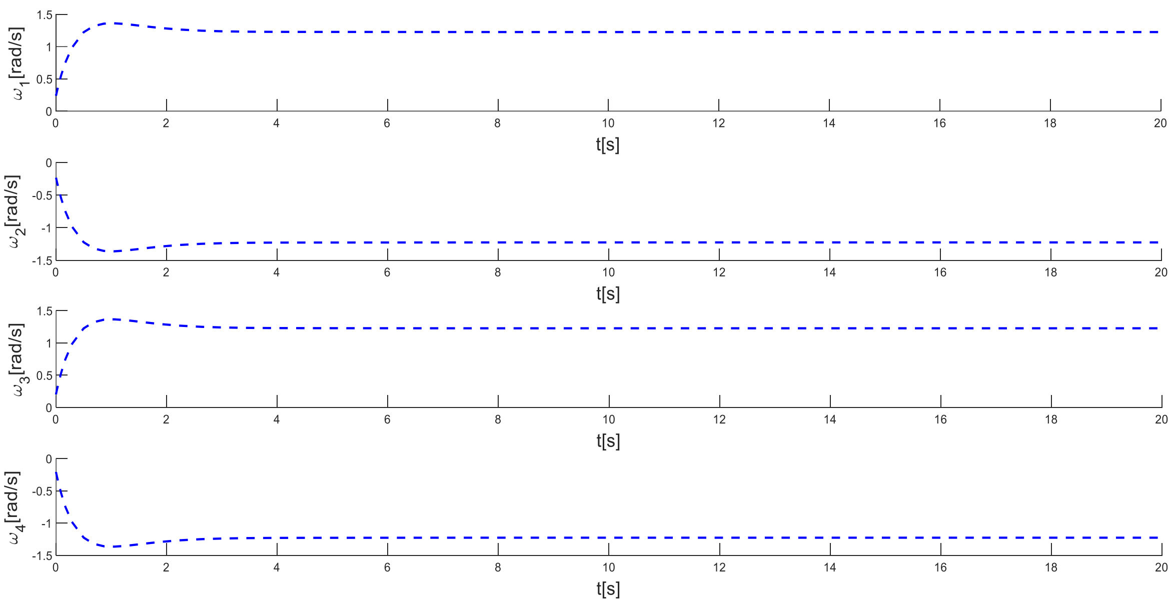

Figure 4. Angular velocity of the rotors

3.2. Test 2 (second rotor failure without disturbance)

In this test, the second rotor was assumed to be faulty while there is no disturbance in the system, as depicted in Figure 5. As shown in Figures 6 and 7, the system has reached the desired values and has been stabilized; moreover. It has a proper performance in comparison with the case in which the system is working without failure.

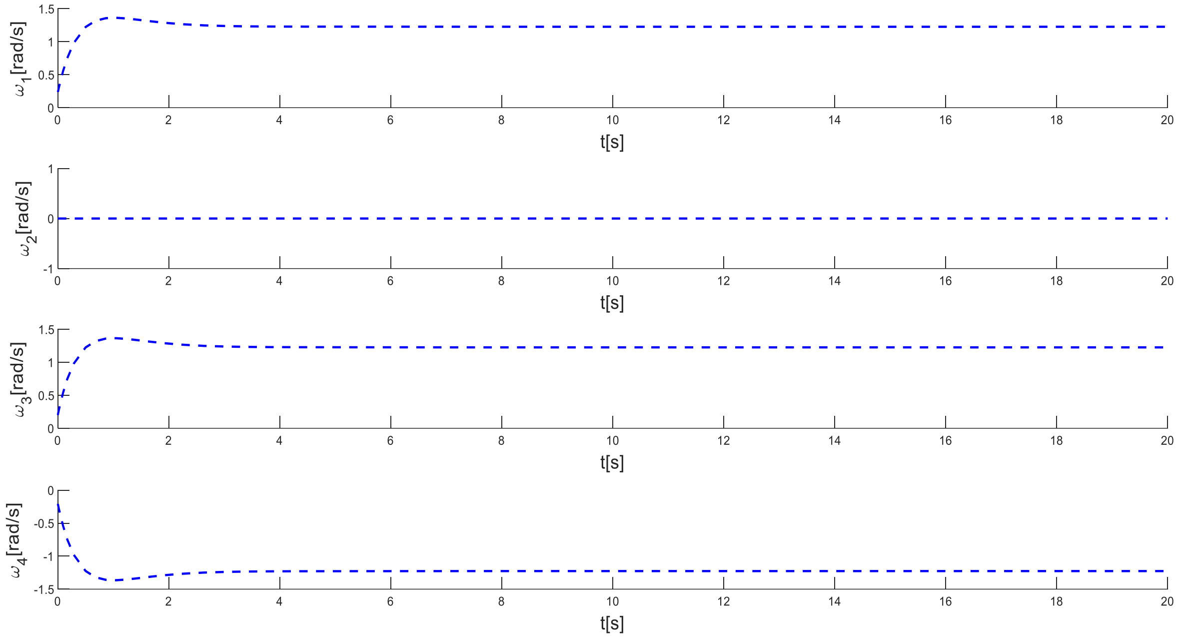

Figure 5. Angular velocity of the rotors

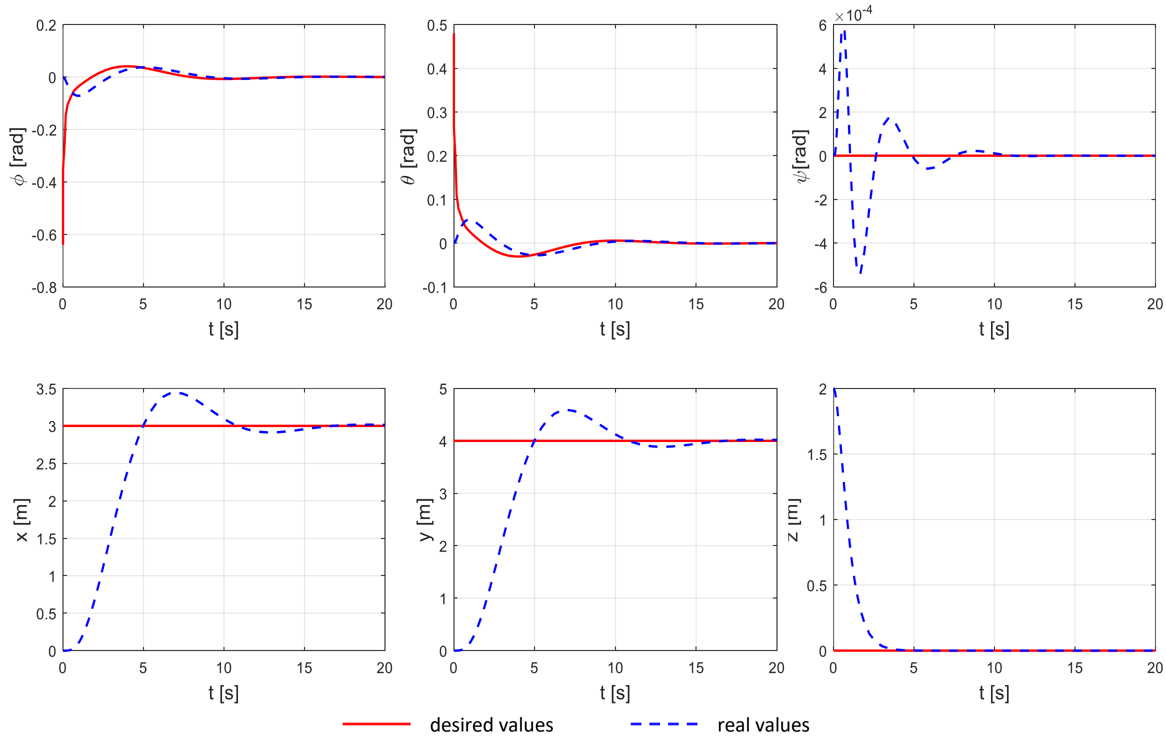

Figure 6. Position and Euler angles

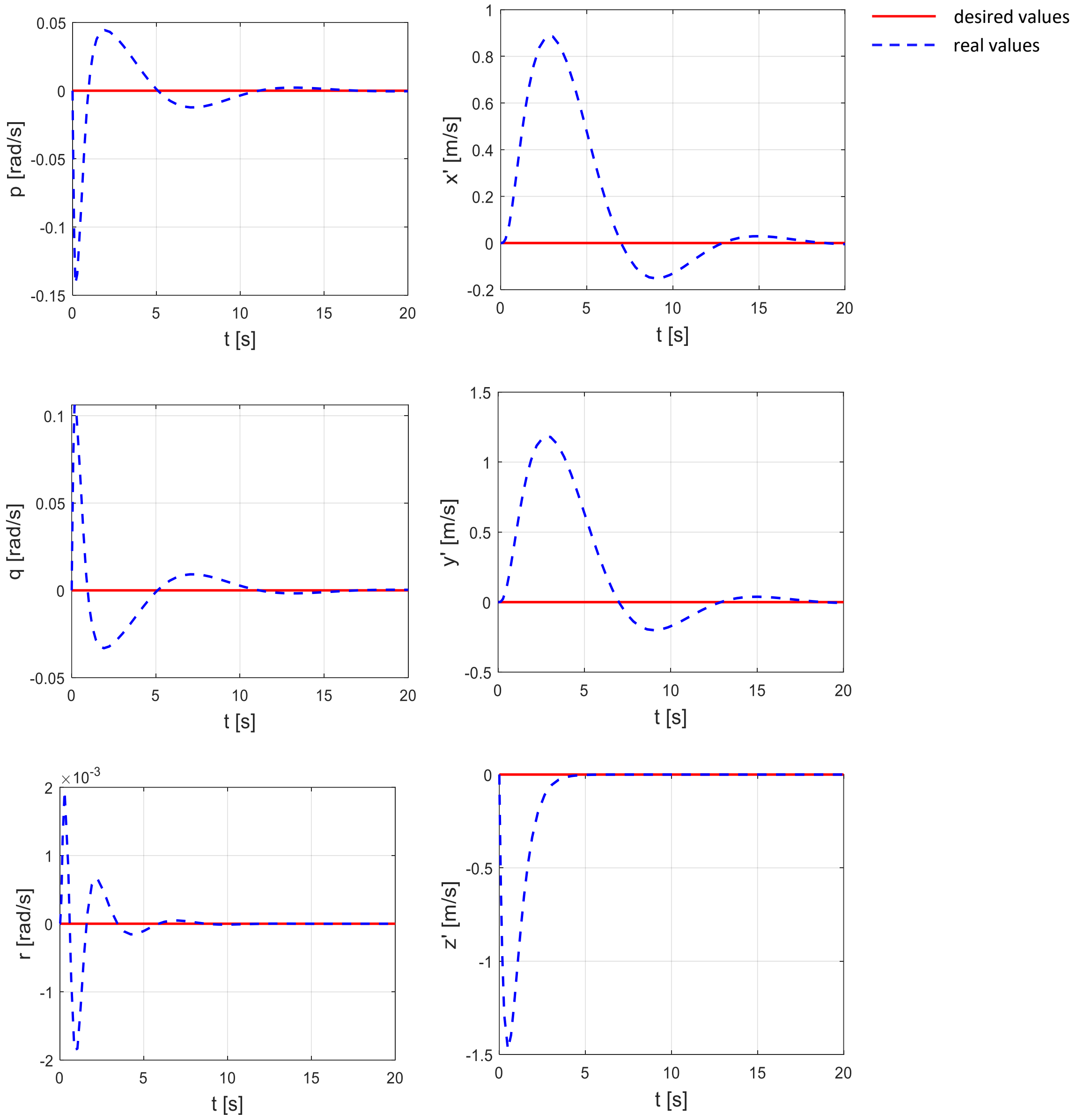

Figure 7. Linear and angular velocity

3.2. Test 3 (second rotor failure with disturbance)

In this test, the second rotor was assumed to be faulty but unlike the above section, disturbance in the system was considered in the form of (28) and (29).

$$d_x = d_y = d_z = 0.02\cos(\pi t) \tag{28}$$

$$d_\varphi = d_\theta = d_\psi = 0.02\sin(\pi t) \tag{29}$$

As shown in Figures 8 and 9, the system has reached the desired values despite the disturbance. Moreover, it has been stabilized and has a proper performance in comparison with the previous case. The rotor's angular velocity is shown in Figure 10, based on the assumption, the second rotor has failed from the beginning.

As shown in all simulations, the z value reaches its desired value in less than 5 seconds while the x and y values reach theirs in 15 seconds. The rationale for this difference is because of the faster inner control is in z. Moreover, the linear and angular system velocities converged and stabilized toward zero.

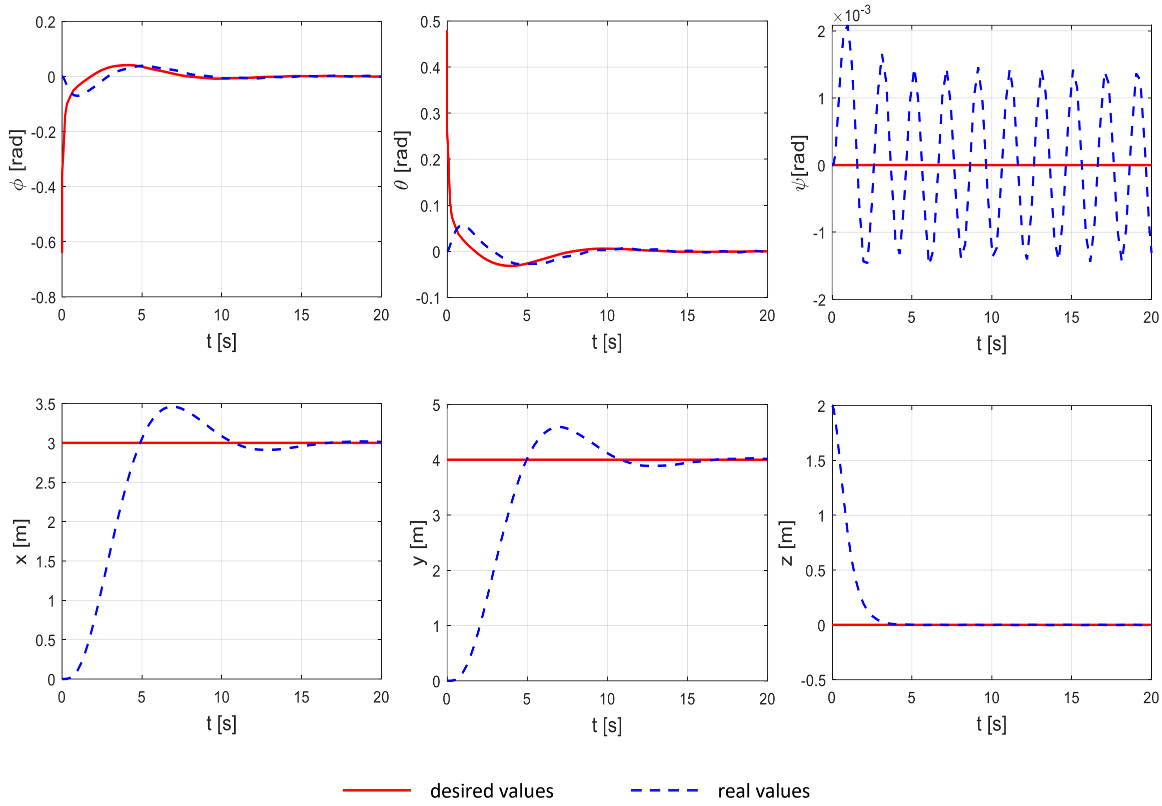

Figure 8. Position and Euler angles

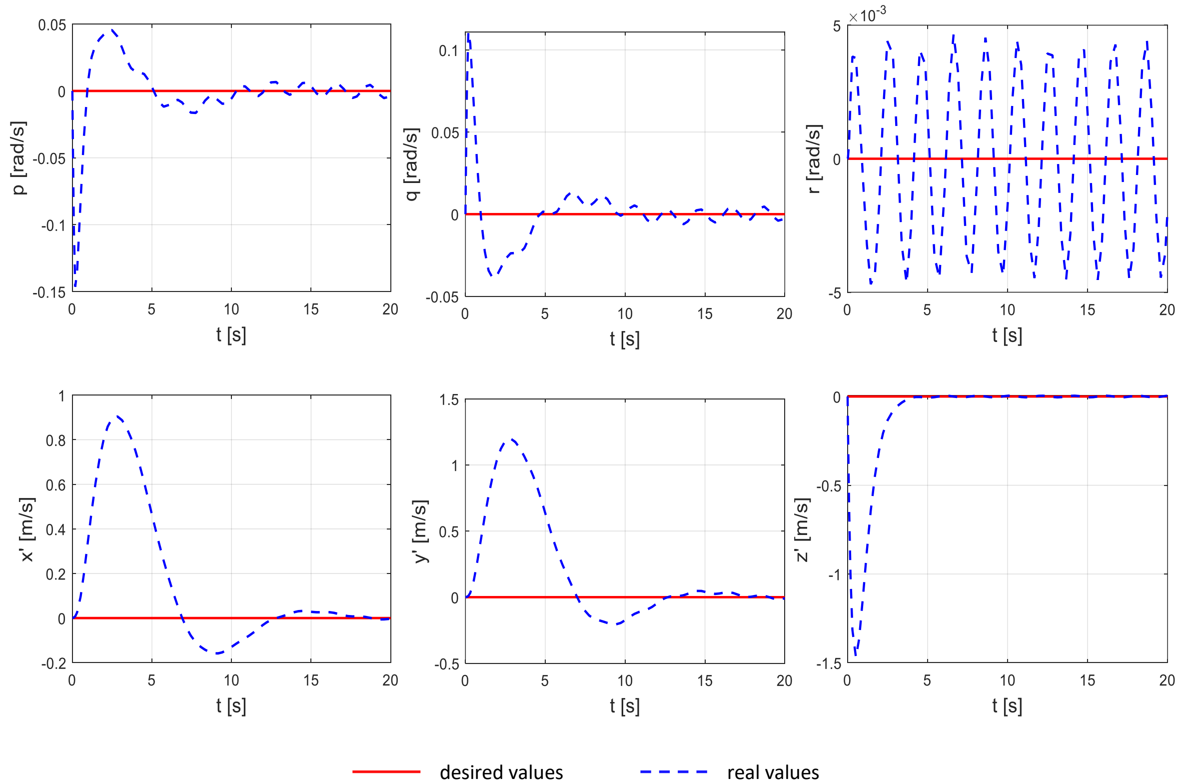

Figure 9. Linear and angular velocity

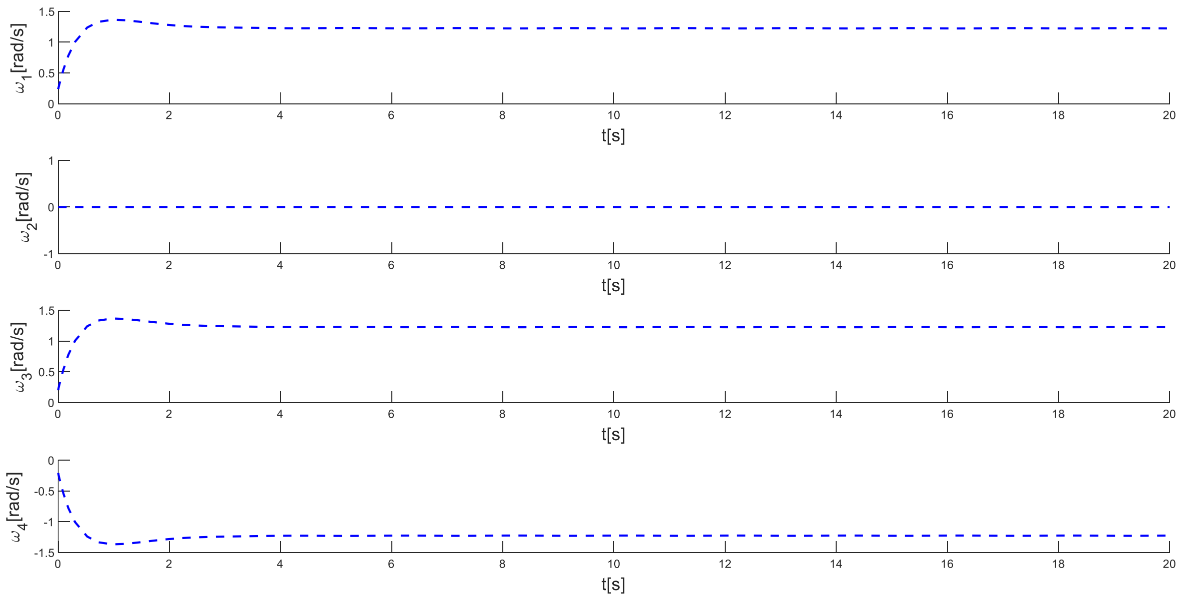

Figure 10. Angular velocity of the rotors

4. CONCLUSION

Efficient flight control of unmanned aerial vehicles is critical to maintain their stability. Since rotor failure is one of the major problems in such systems, this paper addressed this issue by considering first a nonlinear model for the quadcopter and then a state space model for the system. This was achieved through the feedback linearization method, in which the gyroscopic effects because of the rotation of the propeller were not taken into account. Next, using the state space model and the feedback linearization method, a fault-tolerant controller was designed based on the dual control loop structure.

To check the control system's performance, simulations with three different scenarios were implemented, and the results demonstrated the reliability of the proposed approach since, despite a rotor failure and disturbance of the fault-tolerant controller, the state variables converge to their reference values and the quadcopter is capable of completing its mission with only three rotors and without affecting its position.

REFERENCES

[1] J.-J. Xiong and G.-B. Zhang, "Global fast dynamic terminal sliding mode control for a quadrotor UAV," *ISA Transactions*, vol. 66, pp. 233–240, Jan. 2017, doi: 10.1016/j.isatra.2016.09.019.

[2] N. Ben Ammar, S. Bouallègue, J. Haggège, and S. Vaidyanathan, "Chattering free sliding mode controller design for a quadrotor unmanned aerial vehicle," 2017, pp. 61–79. doi: 10.1007/978-3-319-55598-0_3.

[3] V. Lippiello, F. Ruggiero, and D. Serra, "Emergency landing for a quadrotor in case of a propeller failure: A backstepping approach," in *2014 IEEE/RSJ International Conference on Intelligent Robots and Systems*, Sep. 2014, pp. 4782–4788. doi: 10.1109/IROS.2014.6943242.

[4] G. Antonelli, E. Cataldi, F. Arrichiello, P. Robuffo Giordano, S. Chiaverini, and A. Franchi, "Adaptive trajectory tracking for quadrotor MAVS in presence of parameter uncertainties and external disturbances," *IEEE Transactions on Control Systems Technology*, vol. 26, no. 1, pp. 248–254, Jan. 2018, doi: 10.1109/TCST.2017.2650679.

[5] M. Labbadi and M. Cherkaoui, "Robust adaptive backstepping fast terminal sliding mode controller for uncertain quadrotor UAV," *Aerospace Science and Technology*, vol. 93, p. 105306, Oct. 2019, doi: 10.1016/j.ast.2019.105306.

[6] R. Miranda-Colorado and L. T. Aguilar, "Robust PID control of quadrotors with power reduction analysis," *ISA Transactions*, vol. 98, pp. 47–62, Mar. 2020, doi: 10.1016/j.isatra.2019.08.045.

[7] R. Fessi and S. Bouallègue, "LQG controller design for a quadrotor UAV based on particle swarm optimisation," *International Journal of Automation and Control*, vol. 13, no. 5, p. 569, 2019, doi: 10.1504/IJAAC.2019.101910.

[8] P. Lu and E.-J. van Kampen, "Active fault-tolerant control for quadrotors subjected to a complete rotor failure," in *2015 IEEE/RSJ International Conference on Intelligent Robots and Systems (IROS)*, Sep. 2015, pp. 4698–4703. doi: 10.1109/IROS.2015.7354046.

[9] X. Zhang, Y. Zhang, C.-Y. Su, and Y. Feng, "Fault-tolerant control for quadrotor UAV via backstepping approach," Jan. 2010. doi: 10.2514/6.2010-947.

[10] Z. Hou, P. Lu, and Z. Tu, "Nonsingular terminal sliding mode control for a quadrotor UAV with a total rotor failure," *Aerospace Science and Technology*, vol. 98, p. 105716, Mar. 2020, doi: 10.1016/j.ast.2020.105716.

[11] F. Sharifi, M. Mirzaei, B. W. Gordon, and Y. Zhang, "Fault tolerant control of a quadrotor UAV using sliding mode control," in *2010 Conference on Control and Fault-Tolerant Systems (SysTol)*, Oct. 2010, pp. 239–244. doi: 10.1109/SYSTOL.2010.5675979.

[12] Y. Aoki, Y. Asano, A. Honda, N. Motooka, and T. Ohtsuka, "Nonlinear model predictive control of position and attitude in a hexacopter with three failed rotors," *IFAC-PapersOnLine*, vol. 51, no. 20, pp. 228–233, 2018, doi: 10.1016/j.ifacol.2018.11.018.

[13] H. A. Izadi, Y. Zhang, and B. W. Gordon, "Fault tolerant model predictive control of quad-rotor helicopters with actuator fault estimation," *IFAC Proceedings Volumes*, vol. 44, no. 1, pp. 6343–6348, Jan. 2011, doi: 10.3182/20110828-6-IT-1002.03709.

[14] F. Nan, S. Sun, P. Foehn, and D. Scaramuzza, "Nonlinear MPC for quadrotor fault-tolerant control," *IEEE Robotics and Automation Letters*, vol. 7, no. 2, pp. 5047–5054, Apr. 2022, doi: 10.1109/LRA.2022.3154033.

[15] R. C. Avram, X. Zhang, and J. Muse, "Nonlinear adaptive fault-tolerant quadrotor altitude and attitude tracking with multiple actuator faults," *IEEE Transactions on Control Systems Technology*, vol. 26, no. 2, pp. 701–707, Mar. 2018, doi: 10.1109/TCST.2017.2670522.

[16] D. Asadi, K. Ahmadi, and S. Y. Nabavi, "Fault-tolerant trajectory tracking control of a quadcopter in presence of a motor fault," *International Journal of Aeronautical and Space Sciences*, vol. 23, no. 1, pp. 129–142, Feb. 2022, doi: 10.1007/s42405-021-00412-9.

[17] C. D. Pose, J. I. Giribet, and A. S. Ghersin, "Hexacopter fault tolerant actuator allocation analysis for optimal thrust," in *2017 International Conference on Unmanned Aircraft Systems (ICUAS)*, Jun. 2017, pp. 663–671. doi: 10.1109/ICUAS.2017.7991321.

[18] F. Fei, Z. Tu, D. Xu, and X. Deng, "Learn-to-recover: retrofitting UAVs with reinforcement learning-assisted flight control under cyber-physical attacks," in *2020 IEEE International Conference on Robotics and Automation (ICRA)*, May 2020, pp. 7358–7364. doi: 10.1109/ICRA40945.2020.9196611.

[19] M. Saied, M. Knaiber, H. Mazeh, H. Shraim, and C. Francis, "BFA fuzzy logic based control allocation for fault-tolerant control of multirotor UAVs," *The Aeronautical Journal*, vol. 123, no. 1267, pp. 1356–1373, Sep. 2019, doi: 10.1017/aer.2019.58.

[20] A. Jebelli, M. C. E. Yagoub, and B. S. Dhillon, "Feedback linearization approach to fault tolerance for a micro quadrotor," in *2018 IEEE International Conference on Industrial Technology (ICIT)*, Feb. 2018, pp. 165–168. doi: 10.1109/ICIT.2018.8352170.

[21] A. Freddi, A. Lanzon, and S. Longhi, "A feedback linearization approach to fault tolerance in quadrotor vehicles," *IFAC Proceedings Volumes*, vol. 44, no. 1, pp. 5413–5418, Jan. 2011, doi: 10.3182/20110828-6-IT-1002.02016.

[22] A. Jebelli, M. C. E. Yagoub, and B. S. Dhillon, "Design and control of a self-balancing autonomous underwater vehicle with vision capabilities," Journal of Marine Science: Research & Development, Vol. 8, No. 1, 2018, pp. 1-7, 2018. doi: 10.4172/2155-9910.1000245.

BIOGRAPHIES OF AUTHORS

Ali Jebelli received his master's degree and Ph.D. in electrical and computer engineering from the University of Ottawa in 2014 and 2016. During his studies at the University of Ottawa, he worked as a research assistant and teacher assistant in the Department of Mechanical Engineering and the School of Electrical Engineering and Computer Science, and during that time, he won several prestigious awards. He also received a master's degree (M.Eng.) in electrical–mechatronics and automatic control from the University Technology Malaysia in 2009, and his bachelor's degree in electrical power engineering in 2005. His research interests include autonomous systems, intelligent control, robotics, mechatronics, electric motors drive, and solar and wind energy. He has authored or co-authored over 100 publications on these topics in international journals and referred conferences. Dr. Jebelli is currently leading the RoboticC Inc group, a team interested in building agricultural robots to increase the quality and quantity of products and designing autonomous vehicles and drones. Prior to this position, he completed three post-doctoral positions: the first with the Departments of Electrical Engineering and Computer Science and Mechanical Engineering at the University of Ottawa and the second with the Department of Electronics at Carleton University, and the third with the Department of Mechanical Engineering at the University of Alberta. He can be contacted at jebelli@ualberta.ca.

Alireza Najafiyanfar received his B.Sc. degree in control engineering from Tafresh University in 2018, and his M.S. degree in control engineering from K.N. Toosi University of Technology, Tehran, Iran in 2021. His research interests are hybrid systems, symbolic control, system identification, nonlinear control, intelligence control, industrial automation, autonomous robotics, and electric motor drives. He can be contacted at najafiyanfar@email.kntu.ac.ir.

Arezoo Mahabadi is currently a graduate student at Shahed University. Arezoo received her B.Eng. degree with Honors in basic engineering science from the University of Tehran in 2019. Her research interests include intelligent systems, robotics, mechatronics, mathematical modeling of stationary fields, computational electromagnetics solar energy systems, sonar and radar systems, electric motor drives, and energy storage and management. She is currently the supervisor of the engineering department at RoboticC Inc. She can be contacted at a.mah.abadi@ut.ac.ir.

Mustapha C. E. Yagoub received a Dipl.-Ing. degree in electronics and the magister degree in telecommunications, both from the École Nationale Polytechnique, Algiers, Algeria, in 1979 and 1987, respectively, and the Ph.D. degree from the Institut National Polytechnique, Toulouse, France, in 1994. After a few years working in the industry as a design engineer, he joined the Institute of Electronics, Université des Sciences et de la Technologie Houari Boumédiene, Algiers, Algeria, first as a lecturer during 1983-1991 and then as an assistant professor during 1994-1999. From 1996 to 1999, he has been the head of the communication department. From 1999 to 2001, he was a visiting scholar with the Department of Electronics, Carleton University, Ottawa, ON, Canada, working on neural network applications in microwave areas. In 2001, he joined the School of Electrical Engineering and Computer Science (EECS), University of Ottawa, Ottawa, ON, Canada, where he is currently a professor. He has authored or co-authored over 300 publications on these topics in international journals and referred conferences. He authored Conception de Circuits Linéaires Et Non Linéaires Micro-Ondes (Cépadues, Toulouse, France, 2000), and co-authored Computer Manipulation and Stock Price Trend Analysis (Heilongjiang Education Press, Harbin, China, 2005). Dr. Yagoub is a senior member of the IEEE Microwave Theory and Techniques Society, a member of the Professional Engineers of Ontario, Canada, and a member of the Ordre des Ingénieurs du Québec, Canada. He can be contacted at myagoub@uottawa.ca.